Acta Cryst. (1997). B53, 364–372

Structure of Mn_8Sn_5

MARGARETA ELDING-PONTÉN,[a] LARS STENBERG,[a] SVEN LIDIN,[b]* GOTZON MADARIAGA[c] AND JUAN-MANUEL PÉREZ MATO[c]

[a]*Inorganic Chemistry 2, Lund University, PO Box 124, S-221 00 Lund, Sweden,* [b]*Inorganic Chemistry, Arrhenius Laboratory, Stockholm University, S-106 91 Stockholm, Sweden, and* [c]*Departamento de Física de la Materia Condensada, Facultad de Ciencias, Universidad del Pais Vasco, Apdo 644, Bilbao, Spain. E-mail: sven@inorg.su.se*

(Received 11 October 1996; accepted 7 January 1997)

Abstract

The title compound crystallizes as a slightly incommensurate modulation of the B8-type structure. In a basic NiAs structure, ~60% of the trigonal pyramidal interstices are filled with Mn atoms in an ordered manner. The highest corresponding commensurate space group is *Pbnm* (*Pnma*, no. 62) with the cell parameters $a = 21.9114\ (4)$, $b = 7.6003\ (5)$, $c = 5.5247\ (5)$ Å. The four-dimensional superspace group of the incommensurate structure is $Cmcm(\alpha 00)0s0$ (no. 63.8), with the conventional setting $Amam(00\gamma)0s0$. The cell parameters for this incommensurate cell are $a = 382\ (1)$, $b = 7.600\ (2)$, $c = 5.525\ (2)$ Å, $\mathbf{q} = [0.616\ (5), 0, 0]$. The structural refinements were carried out on a multiply twinned specimen. The R factors were 0.037 for the incommensurate refinement and 0.046 for one commensurate approximation. The refinements unambiguously show that the modulation is caused by the step-like modulation of one Mn site, which is accompanied by small displacive modulations of the basic lattice. The incommensurate nature of the modulation is manifested in a slight splitting of fifth-order satellites, visible in electron diffraction.

1. Introduction

The Mn–Sn system contains three binary phase regions; $MnSn_2$ with the $CuAl_2$-type structure, Mn_3Sn with the Ni_3Sn-type structure and an extended B8-type structure field at ~60–70% Mn. In a recent study (Elding-Pontén, Stenberg, Larsson, Lidin & Ståhl, 1997), it was shown that this is a phase bundle containing at least three distinct phases. All phases are intermediates between the NiAs- and Ni_2In-type structures; Sn in hexagonal close packing and Mn in all octahedral interstices form the NiAs-type structure, while the remaining Mn occupy part of the trigonal bipyramidal interstices according to different ordered modes in the three phases of the bundle. The resulting distortion of the basic hexagonal lattice is slight and, consequently, twinning is rife. The present study deals with the effectively incommensurate modulated structure of the phase designated HTP2 (second high-temperature phase). The modulation vector of this phase is very close to 3/10(110)* (hexagonal setting).

2. Experimental

Manganese powder (Goodfellow Metals 99.9%) and tin grains (Kistner 99.5%) in the molar ratio 3:2 were pressed into a pellet and arc-melted under argon. The resulting ingot was crushed, sealed in silica under vacuum and annealed at 1073 K for 2.5 weeks. The sample was left to cool to room temperature in the oven (*ca* 100 K h^{-1}). From this synthesis, crystal fragments were picked, placed on a bed of powdered ZnO, sealed in silica tubes under vacuum, annealed at 573 K for 3 weeks and subsequently quenched in ice water. The ZnO bed was used to keep the crystals separated in order to monitor expulsion of Sn or Mn. EDX analysis detected no Zn in the crystals thus treated.

A multiply twinned crystal was used for the data collection. Owing to the merohedral twinning, the base structure reflections overlap so that each base reflection contains contributions from three distinct crystallite orientations, while the superstructure reflections are non-overlapping and may be measured independently. To discard the strong twinned base lattice reflections and base a refinement solely on the satellite reflections, as has been done previously in other systems (Larsson, Stenberg & Lidin, 1994), seems inadvisable in this case, since the number of observable satellites in the X-ray measurement is strictly limited to the first and second orders, while in the electron diffraction pattern (Fig. 1) it is possible to discern up to five orders of satellites. The twinned data were, therefore, deconvoluted using a twin refinement program and the resulting data set was used in the beginning of the incommensurate refinement of the structure.

The data collection parameters are given in Table 1. The deviation of the **q** vector from 3/10(110)* is sufficiently small to allow the approximation of the

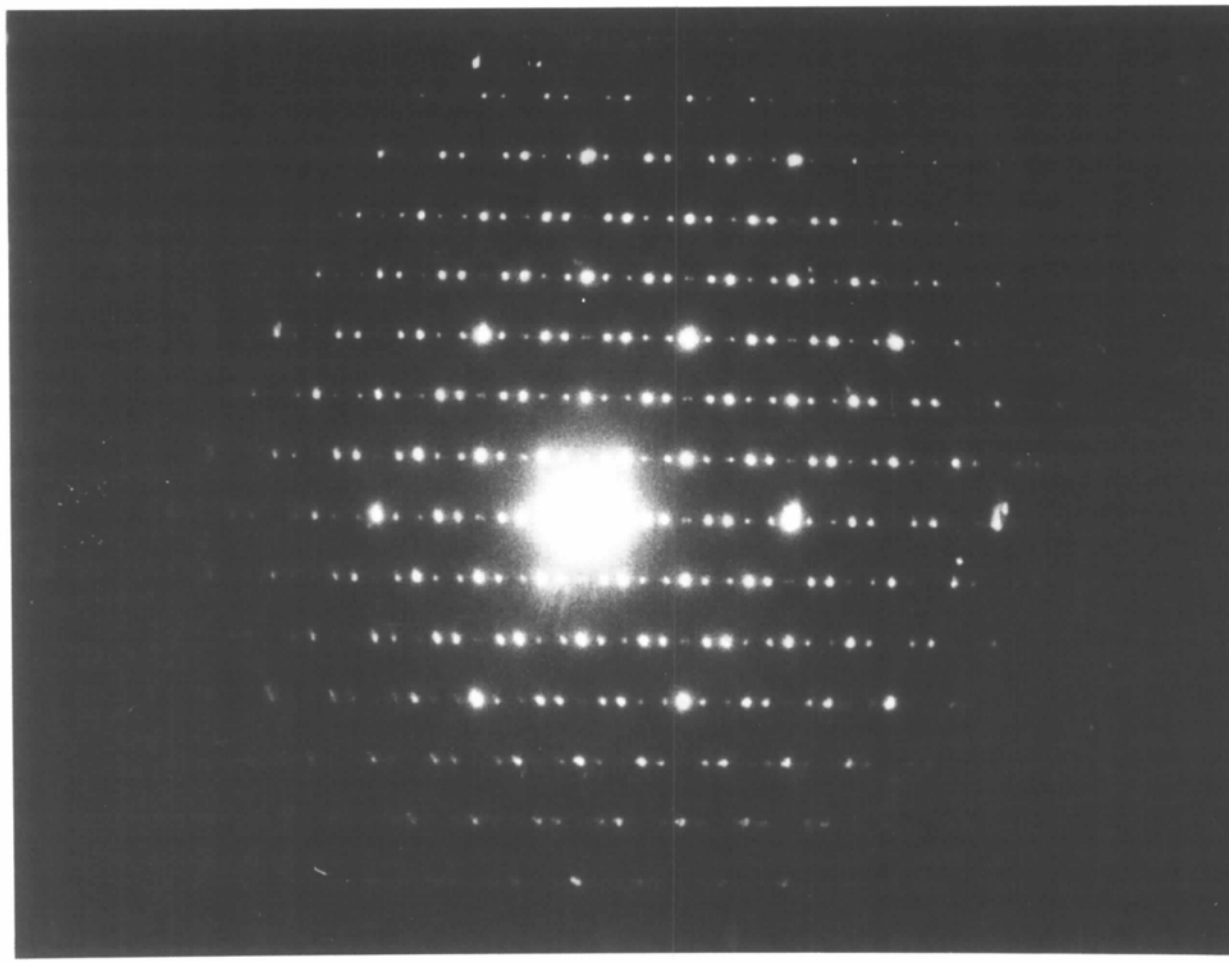

(*a*)

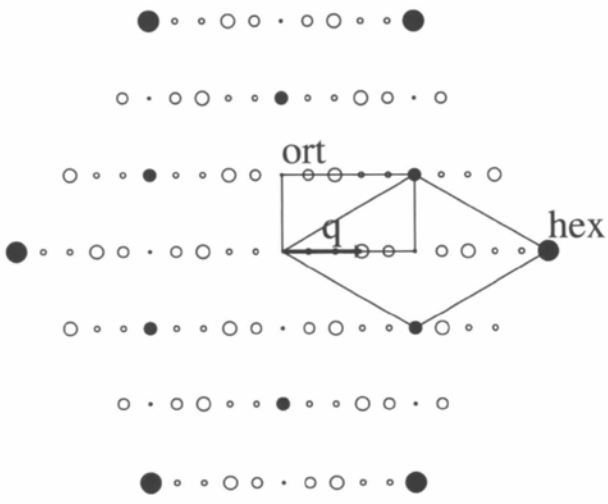

(*b*)

Fig. 1. (*a*) Electron diffraction patterns from Mn_8Sn_5. The zone axis is $[001]_{hex} = [001]_{ort}$. (*b*) Drawing of the enlarged central part of the diffraction pattern. Reflections of the hexagonal basic lattice are filled circles, open circles are satellites. The hexagonal unit cell and the orthorhombic mean cell are indicated together with the **q** vector. It is clear that $\mathbf{q} \simeq 3/10(110)^*_{hex} \simeq 3/5(100)^*_{ort}$.

incommensurate lattice by an orthorhombic commensurate cell ($a = 21.9114, b = 7.6003, c = 5.5247$ Å). This is generated by the action of the matrix

$$M = \begin{bmatrix} 5 & 5 & 0 \\ \bar{1} & 1 & 0 \\ 0 & 0 & 1 \end{bmatrix}$$

on the basic hexagonal unit cell. The error in the **q** vector was estimated from electron diffraction, where the deviation from commensurability could be seen directly as a splitting of fifth-order satellites.

In order to overcome difficulties with absorption, a full sphere of data was collected. For a small inner sphere, the intensities of the satellite reflections were measured for all three possible orientations of the superstructure cell. The data sets were used to calculated the volume ratio for the three orientations, yielding an average intensity ratio of 1.00:0.18:0.08, corresponding to a volume ratio of 1.00:0.42:0.29. Data reduction, Lorentz, polarization and absorption corrections were carried out using the *TEXSAN* (Molecular Structure Corporation, 1993) software package.

The X-ray data set showed the systematic absences $0kl, k \neq 2n$; $h0l, h + l \neq 2n$ compatible with space group *Pbnm*. In the four-dimensional indexing generated by $h = 5h' + m'$, $m \in \{-2, -1, 0, 1, 2\}$, $k' = k$, $l' = l$, the conditions for observed reflections become $hklm$, $h + k = 2n$; $h0lm$, $l + m = 2n$; the former condition partially coinciding with the conditions for the three-dimensional b glide and the latter recuperating the n glide. The extinctions in four dimensions are indicative of the superspace group $Cmcm(\alpha 00)0s0$. A more detailed account of superspace-group–space-group considerations is given in Appendix *A*.

3. Commensurate refinement in space group *Pbnm*

As a starting model, the structure was assumed to consist of a basic NiAs-type arrangement, with Sn forming a hexagonally close-packed arrangement and an equimolar amount of Mn (1–3) occupying all octahedral interstices, the remaining Mn (*A*–*C*) partially filling the trigonal bipyramidal interstices in an ordered manner (Elding-Pontén, Stenberg, Larsson, Lidin & Ståhl, 1997).

The twin program *Mehrling* (Eitel & Bärnighausen, 1985) was used for the refinement. Not surprisingly, the structure proved rather difficult to refine owing to strong correlations between the atomic positions. By refining only two atoms at a time, the unweighted R value was brought down from 0.25 to 0.12. By setting the isotropic displacement factors equal for equal types of atoms and refining these displacements together with all positional parameters, the R factor was reduced to 0.064. It was not possible to refine the individual isotropic displacement factors because of severe coupling between the parameters. The program *Mehrling* is useful for deconvoluting twin data but does not allow for the calculation of $\Delta\rho$ maps and the deconvoluted data were therefore used as input into *SHELXL*93 (Sheldrick, 1993). Here, those data were averaged and final parameters calculated. Owing to the averaging, the agreement factor decreased further to $R = 0.046$. The result of the refinement is shown in Tables 2 and 3.* Using satellite reflections only leads to an even lower R factor (0.04), a significant decrease in the $(\Delta\rho)_{\min,\max}$ values (by a factor of 2), less correlation between the parameters for atoms in the higher (parent) symmetry and smaller shifts. This is perfectly consistent with the view that the main reflections carry information chiefly from the parent structure and the satellites from the superstructure, but main reflections and satellites have been treated differently because of twinning. The twinning, together with the high linear absorption coefficient, presents an additional source of inaccuracy; the proportions of domains displaying the three individual directions are not the same and this indicates a relatively low number of large domains, as opposed to a large number of micro-domains. While a micro-twinned specimen may be simply treated as an isotropically diluted crystal in the absorption correction, large domains cause anisotropic shadowing of the satellite reflections. The absorption effects, which are large, are therefore difficult to correct for.

4. Incommensurate refinement

The refinement was carried out using the software package *JANA* (Petříček, 1994). The data corrected for twinning were used in the initial stages of the refinement. First only the basic reflections $hkl0$ were used to refine the average structure, then the full twinned data set was introduced. The average structure contains only three independent atomic positions, one of them, Mn2, being partially occupied. Anisotropic thermal displacement parameters of the basic structure were refined and then positional modulations were introduced. The occupational modulation of Mn2 was first modelled by sinusoidal functions, but an analysis of the modulation showed this to be quite square, as might be expected from the commensurate refinement. The modulation was then modelled with a square-wave crenel function (Petříček, van der Lee & Evain, 1995). The final value for the width of the crenel function, 0.62, corresponds to a 62% occupation of that site in the mean structure. The deviation from the nominal composition Mn_8Sn_5 is thus within the experimental

*A list of structure factors has been deposited with the IUCr (Reference: AB0366). Copies may be obtained through The Managing Editor, International Union of Crystallography, 5 Abbey Square, Chester CH1 2HU, England.

Table 1. *Experimental details*

	Commensurate refinement	Data applicable to both refinements	Incommensurate refinement
Crystal data			
Chemical formula		Mn_8Sn_5	
Chemical formula weight		1032.96	
Cell setting		Orthorhombic	
Space group	*Pbnm*		*Cmcm*(α00)0s0
a (Å)	21.9114 (4)		4.3822 (1)
b (Å)		7.6003 (5)	
c (Å)		5.5247 (5)	
V (Å^3)/**q**	920.05 (10)		0.616, 0, 0
Z	4		–
D_x (Mg m^{-3})		7.46	
Radiation type		Mo $K\alpha$	
Wavelength (Å)		0.70926	
No. of reflections for cell parameters		20	
θ range (°)		6.5–23.5	
μ (mm^{-1})		23.5	
Temperature (K)		293 (2)	
Crystal form		Fragment	
Crystal size (mm)		0.05 × 0.03 × 0.015	
Crystal colour		Grey, metallic	
Data collection			
Diffractometer		Enraf–Nonius CAD-4	
Data collection method		ω–2θ scans	
Absorption correction		Analytical from shape	
T_{min}		0.5515	
T_{max}		0.8242	
No. of measured reflections		16103	
No. of independent reflections		2359	
No. of observed reflections		400	
Criterion for observed reflections		$I > 2\sigma(I)$	
R_{int}		0.0940	
θ_{max} (°)		34.84	
Range of *h*, *k*, *l*	$-12 \rightarrow h \rightarrow 12$ $-8 \rightarrow k \rightarrow 8$ $-35 \rightarrow l \rightarrow 35$		Main reflections 136 First order 201 Second order 63
No. of standard reflections		3	
Frequency of standard reflections (min)		60	
Intensity decay (%)		1.9	
Refinement			
Refinement on	F^2		F
$R[F^2 > 2\sigma(F^2)]$	0.046		0.037
$wR(F^2)$	0.121		R_0 = 3.32; R_1 = 3.77; R_2 = 5.63
S	1.63		2.6
No. of reflections used in refinement		400	
No. of parameters used	25		36
Weighting scheme	$w = 1/[\sigma^2(F_o^2) + (0.0555P)^2]$, where $P = (F_o^2 + 2F_c^2)/3$		$w = 1/\sigma^2(F_0)$
$(\Delta/\sigma)_{max}$	4.717		<0.01
$\Delta\rho_{max}$ (e Å^{-3})	5.222		3.06
$\Delta\rho_{min}$ (e Å^{-3})	−2.524		−3.84
Extinction method	None		
Source of atomic scattering factors		*International Tables for Crystallography* (1992, Vol. C, Tables 4.2.6.8 and 6.1.1.4)	
Computer programs			
Structure solution		*SHELXS*86 (Sheldrick, 1990)	
Structure refinement	*SHELXL*93 (Sheldrick, 1993)		*JANA* (Petricek, 1994)

accuracy. The refinement was quite straight-forward, the only information used from the commensurate approximation was, apart from the mean structure, the fact that the positional modulation of Sn appeared to be rather anharmonic. Thus, sixth-order harmonics were introduced to deal with this particular modulation. For the Mn1 atom, two harmonics were used for the positional modulation along *y* and *z* axes and a single term for the Mn2 atom. Final values for the parameters refined are found in Table 4. The modulation functions

Table 2. *Fractional atomic coordinates and equivalent isotropic displacement parameters ($Å^2$) for the Pbnm model*

$$U_{eq} = (1/3)\Sigma_i\Sigma_j U^{ij} a_i^* a_j^* \mathbf{a}_i.\mathbf{a}_j.$$

	Wyckoff position	x	y	z	U_{eq}
Mn1	4(*a*)	0.0000	0.0000	0.0000	0.0081 (4)
Mn2	8(*d*)	0.203 (2)	−0.018 (1)	−0.005 (3)	0.0081 (4)
Mn3	8(*d*)	0.402 (3)	0.020 (1)	0.000 (2)	0.0081 (4)
Sn1	4(*c*)	0.0151 (2)	0.3068 (6)	3/4	0.0069 (3)
Sn2	4(*c*)	0.1914 (2)	0.3217 (6)	3/4	0.0069 (3)
Sn3	4(*c*)	0.3986 (4)	0.3717 (3)	3/4	0.0069 (3)
Sn4	4(*c*)	0.6164 (2)	0.3047 (5)	3/4	0.0069 (3)
Sn5	4(*c*)	0.7949 (2)	0.3451 (5)	3/4	0.0069 (3)
Mn*A*	4(*c*)	0.001 (1)	0.335 (2)	1/4	0.0081 (4)
Mn*B*	4(*c*)	0.397 (1)	0.342 (1)	1/4	0.0081 (4)
Mn*C*	4(*c*)	0.797 (1)	0.341 (3)	1/4	0.0081 (4)

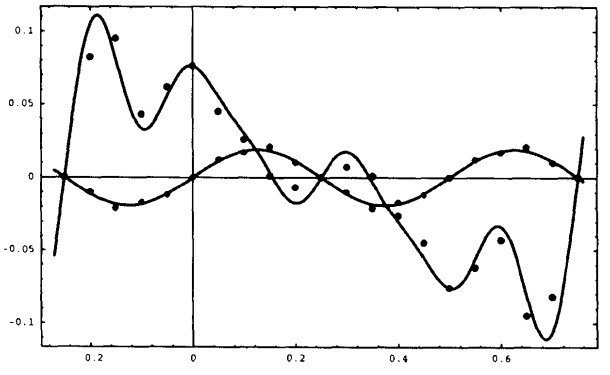

(*a*)

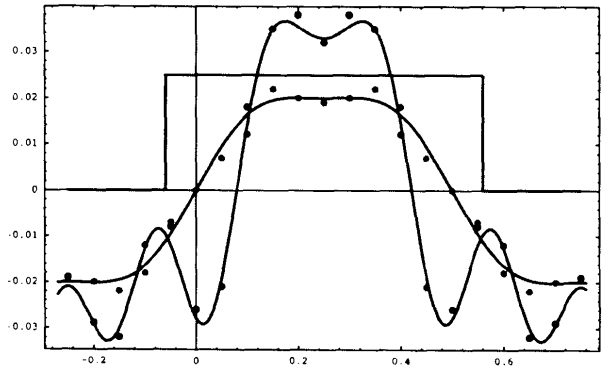

(*b*)

Fig. 2. Atomic modulation functions for Mn_8Sn_5. Positional modulations are shown for Sn and Mn1 only, that for Mn2 being exceedingly weak. The discs correspond to the positions of the atoms in the commensurate approximations. Black discs correspond to Sn, grey to Mn1. The discs at 0.0, 0.1 *etc.* originate from the *Pbnm* approximant, while those at 0.05, 0.15 *etc.* originate from the *Pmnm* approximant. (*a*) x direction; the strong modulation is Sn; (*b*) y direction; the strong modulation is Sn. The shape of the occupational modulation of Mn2 is indicated.

Table 3. *Bond lengths (Å) in the Pbnm model*

N is the number of equivalent distances.

	Distance	N		Distance	N
Mn*A*			Mn1		
Sn4	2.74 (2)	1	Sn1	2.73 (1)	2
Sn3	2.74 (1)	1	Sn3	2.79 (1)	2
Sn1	2.74 (1)	1	Sn4	3.26 (1)	2
Sn1	2.79 (1)	2	Mn1	2.76 (1)	2
Mn3	2.80 (6)	2			
Mn1	2.90 (1)	2	Mn2		
Mn3	2.90 (5)	2	Sn3	2.74 (3)	1
			Sn5	2.78 (3)	1
Mn*B*			Sn5	2.86 (1)	1
Sn5	2.64 (2)	1	Sn4	2.87 (2)	1
Sn4	2.70 (1)	1	Sn2	2.93 (1)	1
Sn3	2.77 (1)	2	Sn2	2.94 (3)	1
Sn1	2.83 (1)	1	Mn2	2.70 (3)	1
Mn3	2.81 (2)	2	Mn2	2.82 (3)	1
Mn2	2.81 (3)	2			
Mn1	2.91 (1)	2	Mn3		
			Sn1	2.80 (5)	1
Mn*C*			Sn4	2.85 (1)	1
Sn2	2.58 (2)	1	Sn2	2.90 (5)	1
Sn2	2.63 (2)	1	Sn5	2.91 (6)	1
Sn5	2.76 (1)	2	Sn3	3.01 (1)	1
Sn3	2.75 (2)	1	Sn1	3.13 (6)	1
Mn2	2.80 (2)	2	Mn3	2.76 (2)	1
Mn2	2.81 (3)	2	Mn3	2.77 (2)	1
Mn3	2.88 (6)	2			

are shown in Fig. 2. Final agreement factors were $R = 0.037$, $wR = 0.036$ for 400 independent reflections, $I > 2\sigma(I)$, and $R = 0.032$, $wR = 0.0350$; $R = 0.0377$, $wR = 0.0340$; $R = 0.0563$, $wR = 0.0585$ for main reflections (136); first-order satellites (201); second-order satellites (63), respectively. The residual electron densities were somewhat reduced compared to the commensurate refinement; $\Delta\rho_{min} = -3.84$, $\Delta\rho_{max} = 3.06\,e\,Å^{-3}$. Owing to the orthorhombic averaging, it was not necessary to refine more than one twin ratio. This turned out to be 1.00:0.72, which can be compared to the directly measured value 1.00:0.71.

5. Commensurate refinement in space group *Pmnm*

That attempts to refine the structure in space group *Pmnm* from scratch were unsuccessful was no great surprise. The symmetry constraints of this group on the structure are less restrictive and hence the number of parameters is even larger. After completion of the incommensurate refinement, another attempt was made using the information from the modulation functions. In practice, the ensuing refinement was not straightforward, but still a possible task. From the knowledge of the modulation functions described in Table 4, using the modulation values at the points $\nu = 1/20 + 1/10$ as explained in the Appendix, a commensurate *Pmnm* approximant could be postulated. The model could indeed be refined, but the refinement was even more unstable than in the *Pbmn* model. It was not possible to refine all atomic positions simultaneously and the final R value was 0.015 higher than for the *Pbnm* model. The

Table 4. *Refined values of the parameters of the incommensurate model*

Average structure

	x	y	z	U^{11}	U^{22}	U^{33}	U^{23}
Sn	0	0.3298 (2)	1/4	0.0023 (17)	0.0070 (8)	0.0083 (3)	0
Mn1	0	0	0	0.0075 (11)	0.0099 (10)	0.0046 (11)	−0.0001 (11)
Mn2	0	0.3383 (6)	3/4	0.0113 (14)	0.0075 (15)	0.0119 (9)	0

Atomic positional modulation functions, U, for the incommensurate model

$$U_x^{Sn}(v) = U_{x1}^{Sn}\cos 2\pi v + U_{x2}^{Sn}\sin 4\pi v + U_{x3}^{Sn}\cos 6\pi v + U_{x4}^{Sn}\sin 8\pi v + U_{x5}^{Sn}\cos 10\pi v + U_{x6}^{Sn}\sin 12\pi v$$

$$U_y^{Sn}(v) = U_{y1}^{Sn}\sin 2\pi v + U_{y2}^{Sn}\cos 4\pi v + U_{y3}^{Sn}\sin 6\pi v + U_{y4}^{Sn}\cos 8\pi v + U_{y5}^{Sn}\sin 10\pi v + U_{y6}^{Sn}\cos 12\pi v$$

$$U_x^{Mn1}(v) = U_{x1}^{Mn1}\sin 4\pi v$$

$$U_y^{Mn1}(v) = U_{y1}^{Mn1}\sin 2\pi v + U_{y2}^{Mn1}\sin 6\pi v$$

$$U_z^{Mn1}(v) = U_{z1}^{Mn1}\sin 2\pi v + U_{z2}^{Mn1}\sin 6\pi v$$

$$U_z^{Mn2}(v) = U_{x1}^{Mn2}\cos 2\pi v$$

$$U_y^{Mn2}(v) = U_{y1}^{Mn2}\sin 2\pi v$$

$U_{x1}^{Sn} = 0.062\ (5)$, $U_{y1}^{Sn} = 0.031\ (1)$

$U_{x2}^{Sn} = -0.030\ (1)$, $U_{y2}^{Sn} = -0.013\ (1)$

$U_{x3}^{Sn} = 0.006\ (3)$, $U_{y3}^{Sn} = -0.005\ (1)$

$U_{x4}^{Sn} = 0.032\ (3)$, $U_{y4}^{Sn} = -0.007\ (1)$

$U_{x5}^{Sn} = 0.020\ (2)$, $U_{y5}^{Sn} = -0.009\ (2)$

$U_{x6}^{Sn} = -0.014\ (7)$, $U_{y6}^{Sn} = -0.004\ (1)$

$U_{x1}^{Mn1} = 0.019\ (1)$,

$U_{y1}^{Mn1} = 0.023\ (1)$, $U_{y2}^{Mn1} = -0.003\ (1)$

$U_{z1}^{Mn1} = -0.003\ (1)$, $U_{z2}^{Mn1} = -0.008\ (3)$

$U_{x1}^{Mn2} = 0.006\ (1)$, $U_{y1}^{Mn2} = 0.003\ (1)$

Atomic occupational modulation function, A

$$\begin{cases} v - 0.25 < \Delta^{Mn2}/2, & A^{Mn2}(v) = 1 \\ v - 0.25 > \Delta^{Mn2}/2, & A^{Mn2}(v) = 0 \end{cases}$$

$\Delta^{Mn2} = 0.623\ (4)$

positional parameters of this structural refinement are given in Table 5. No attempt was made to refine the structure in the even less restrictive space group $P2_1nm$. In Fig. 2, the final atomic displacements corresponding to both the *Pbnm* and *Pmnm* approximants are compared to those given by the incommensurate model, showing an excellent agreement.

6. Discussion

Mn_8Sn_5 crystallizes in a superstructure of the NiAs–Ni_2In type, *i.e.* Sn forms a hexagonal close-packed arrangement with Mn in all octahedral interstices. The Sn trigonal bipyramidal interstices are partially occupied by Mn in an ordered manner, giving rise to the superstructure. As in other such phases (Lidin & Larsson, 1995), the trigonal bipyramidal interstices deform by the expansion of the equatorial triangle. The simultaneous relative contraction of the next-nearest-neighbour coordination shell, a trigonal prism of Mn, leads to an effective coordination number of the Mn

Table 5. *Final values for positional parameters for the Pmnm model*

The origin is shifted by $\frac{1}{4}0\frac{1}{4}$ with respect to the origin defined by the point at $2/n$ (origin choice 1).

Atom	Wyckoff position	x	y	z
Mn1	4(*e*)	0	0.019	0.003
Mn2	8(*g*)	0.196	0.988	0.999
Mn3	8(*g*)	0.398	0.007	0.004
Sn1	2(*a*)	0	0.366	3/4
Sn11	2(*b*)	0	0.686	1/4
Sn2	4(*f*)	0.219	0.302	3/4
Sn3	4(*f*)	0.391	0.312	3/4
Sn4	4(*f*)	0.088	0.825	3/4
Sn5	4(*f*)	0.300	0.868	3/4
Mn*A*1	2(*b*)	0	0.352	1/4
Mn*A*2	2(*a*)	0	0.657	3/4
Mn*B*	4(*f*)	0.397	0.338	1/4
Mn*C*	4(*f*)	0.299	0.838	1/4

atoms in these sites of 11 (the Edshammar 11 polyhedron, E_{11}) rather than 5. In similar compounds, the E_{11} polyhedra are often found to be arranged in a manner that minimizes mutual contact, but in this case, owing to the high occupancy (60%) of the E_{11} sites, this is not possible.

The modulation of the title compound is a combination of a compositional and a displacive distortion of the basic lattice. It is evident that the compositional variation is the cause of the correlated displacive modulation that is relatively small (of the order 0.1 Å) compared to the severe effect of the compositional modulation. Nonetheless, the main effect in terms of the intensities of the diffraction pattern emanate from the displacive modulation of the Sn atoms.

The advantages of the incommensurate approach in this study are crystal clear: The incommensurate model incorporates both refined commensurate models as well as the lowest symmetry possibility ($P2_1nm$). The symmetry ambiguity is thus effectively avoided. The model allows for the variations in the **q** vector that may result from small changes in composition, again without symmetry change. The modulation description clearly shows the connection between Mn2 occupancy and base lattice distortions and, finally, and perhaps most convincingly, it gives a smooth and stable refinement of the structure, where all parameters may be let loose simultaneously, while the commensurate approximants refine only when treated with utmost care. The stability difference is easily seen from the $(\Delta/\sigma)_{max}$ values (Table 1), where the *Pbnm* approximation yields a very high value (4.7) while the corresponding value for the incommensurate refinement is virtually zero. The residual electron densities are somewhat high. There are several possible explanations for this; the problem of absorption correction in macro-domain twins has already been mentioned. Another possible source of error is the intergrowth between the different phases in the B8-structure-type field of the Mn–Sn system. It has

been shown (Elding-Pontén, Stenberg, Larsson, Lidin & Ståhl, 1997) that all three B8-type superstructure phases may coexist as domains in specimens that are single crystals with respect to the parent sublattice. The possibility that the specimen used is such a multi-phase single crystal cannot be ruled out. The refined commensurate *Pbnm* approximation of the structure is shown in Fig. 3.

The authors are indebted to Dr V. Petříček for valuable discussions Financial support from the Natural Science Research Council of Sweden (NFR) is gratefully acknowledged.

APPENDIX

Superspace-group–space-group considerations

The choice of space group for the commensurate approximation is not unique; although the extinction conditions ($0kl$: $k \neq 2n$, $h0l$: $h + l \neq 2n$) are perfectly matched, the first condition, corresponding to the *b* glide, applies *only* to satellite reflections of the $5n$th (n is an integer) order and these should be extremely weak if not systematically absent. In the presence of a *b* glide, it is possible to chose the group *Pmnm* or the non-centrosymmetric group $P2_1nm$. The symmetry operators of the superspace group may be deduced from the full symbol $C2/m\,2/c\,2_1/m(\alpha 00)0s0$. Writing the representative operations in the form

{operation|real-space translation **t**, internal translation τ},

we have:

(0) $\{E|000, 0\}$ (1) $\{E|\frac{1}{2}\frac{1}{2}0, 0\}$
(2) $\{I|000, -2\Phi\}$ (3) $\{C_{2x}|000, \frac{1}{2}\}$
(4) $\{C_{2y}|00\frac{1}{2}, \frac{1}{2} - 2\Phi\}$ (5) $\{C_{2z}|00\frac{1}{2}, -2\Phi\}$
(6) $\{\sigma_x|000, \frac{1}{2} - 2\Phi\}$ (7) $\{\sigma_y|00\frac{1}{2}, \frac{1}{2}\}$
(8) $\{\sigma_z|00\frac{1}{2}, 0\}$,

where Φ is the initial phase of the modulation with respect to the inversion centre in internal space. We may now determine which superspace-group operations survive as three-dimensional space-group operations for a commensurate approximant; in this particular case, the special (commensurate) choice is $\mathbf{q} = (\alpha 00) = (3/5\,00)$.

The lattice translations (0) are given by $\{E|\mathbf{t}, -\mathbf{tq}\}$ and this is a three-dimensional lattice translation when τ ($= \mathbf{tq}$) is an integer. It is clear that a periodic lattice is generated by $\{E|500, -3\}$ and thus the cell is pentupled along the x direction. The centring translation (1) is not kept, but it does yield $\{E|\frac{5}{2}\frac{1}{2}0, -\frac{3}{2}\}$ and so operations of the type $\{E|\frac{5}{2}\frac{1}{2}0, -\frac{1}{2}\}\{R|\mathbf{t}, \tau\}$ with $\tau = 1/2$ will be operations of the three-dimensional space group.

Operations that reverse the direction of **q**, *i.e.* the centre of symmetry (2), the reflection (6) and the rotations (4) and (5), are not kept for a general Φ and so the candidates for three-dimensional operations for an arbitrary Φ are (0), (3), (7) and (8), but the centring operation has to be applied to (3) and (7) to remove the *s*-centring term of the modulation.

We are left with

(0) $\{E|000, 0\}$ (3) $\{C_{2x}|\frac{5}{2}\frac{1}{2}0, 0\}$
(7) $\{\sigma_y|\frac{5}{2}\frac{1}{2}\frac{1}{2}, 0\}$ (8) $\{\sigma_z|00\frac{1}{2}, 0\}$,

which corresponds to the space group $P2_1nm$ or, in the standard setting, $Pmn2_1$ (no. 31). This is the minimal symmetry of the commensurate approximation of this phase; special choices of Φ lead to higher symmetry.

For the choice $\Phi = 0$, the restriction that forbids operations (2), (4), (5) and (6) no longer holds and by applying the centring translation to (3), (4), (6) and (7) we obtain

(0) $\{E|000, 0\}$ (2) $\{I|000, 0\}$
(3) $\{C_{2x}|\frac{5}{2}\frac{1}{2}0, 0\}$ (4) $\{C_{2y}|\frac{5}{2}\frac{1}{2}\frac{1}{2}, 0\}$
(5) $\{C_{2z}|00\frac{1}{2}, 0\}$ (6) $\{\sigma_x|\frac{5}{2}\frac{1}{2}0, 0\}$
(7) $\{\sigma_y|\frac{5}{2}\frac{1}{2}\frac{1}{2}, 0\}$ (8) $\{\sigma_z|00\frac{1}{2}, 0\}$

and the space group $P2_1/b\,2_1/n\,2_1/m$ (*Pbnm*) or, in the standard setting, *Pnma* (no. 62). Equivalent space groups are also realized for $\Phi = n/10$, with n an integer, and correspond to the different antiphases with respect to the average *Cmcm* structure. Another

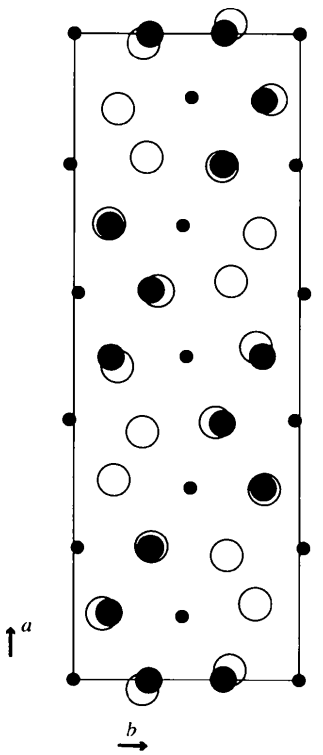

Fig. 3. Approximate *Pbnm* structure of Mn_8Sn_5 projected onto the *ab* plane. Large open circles are Sn, medium sized discs are Mn2 and small discs are Mn1.

possibility to generate a higher three-dimensional symmetry than $P2_1nm$ originates from the choice $\Phi = \frac{1}{4}$. Operations (2), (3), (5) and (7) require the use of the centring translation to obtain a three-dimensional symmetry operation:

(0) $\{E|000, 0\}$ (2) $\{I|\frac{5}{2}\frac{1}{2}0, 0\}$
(3) $\{C_{2x}|\frac{5}{2}\frac{1}{2}0, 0\}$ (4) $\{C_{2y}|00\frac{1}{2}, 0\}$
(5) $\{C_{2z}|\frac{5}{2}\frac{1}{2}\frac{1}{2}, 0\}$ (6) $\{\sigma_x|000, 0\}$
(7) $\{\sigma_y|\frac{5}{2}\frac{1}{2}\frac{1}{2}, 0\}$ (8) $\{\sigma_z|00\frac{1}{2}, 0\}$

and the space group is now $P2_1/m\,2/n\,2_1/m$ (*Pmnm*) or, in the standard setting, *Pmmn* (no. 59). Analogous space groups are again realized for $\Phi = \frac{1}{4} + n/10$.

For an incommensurate structure, the value of Φ is arbitrary and related to the choice of the 'zero' cell along the modulation. The atomic modulation functions describing the structural distortion with respect to the average structure are defined along the internal coordinate v $(= \mathbf{ql} + \mathbf{qr}_0 + \Phi)$, where $\mathbf{l}$ is the cell vector and $\mathbf{r}_0$ is the average position of the atom within the cell. In the following, for the incommensurate superspace description, we chose $\Phi = 0$.

The site symmetry of the atoms in the structure imposes restrictions on the modulation function, just like the constraints on the thermal tensors of the atoms in an ordinary three-dimensional space group. The general form of the positional modulation is

$$U_x(v) = U_{x0} + \sum_{n=1} U^C_{xn} \cos 2\pi n v + U^S_{xn} \sin 2\pi n v$$

with corresponding formulae for U_y and U_z. The atom Mn1 is at the position (0,0,0) in the average structure; the site symmetry is $2/m$ and the individual operations that keep the position invariant are C_{2x}, σ_x and $\bar{1}$. The centre of symmetry sets the conditions

$$U_x(v) = -U_x(-v); \quad U_y(v) = -U_y(-v); \quad U_z(v) = -U_z(-v).$$

U_x is hence an odd function and the constant term and the cosine terms all vanish. The same holds for U_y and U_z. The operation $\{C_{2x}|000, \frac{1}{2}\}$ forces

$$U_x(v) = U_x(v + \tfrac{1}{2}); \quad U_y(v) = -U_y(v + \tfrac{1}{2}); \quad U_z(v) = -U_z(v + \tfrac{1}{2})$$

and all odd terms vanish for x, while even terms vanish for y and z. The mirror plane σ_x does not impose any new restrictions and the modulation for the Mn1 atom takes the form

$$\begin{aligned} U_x(v) &= \sum_{n=1} U^S_{x2n} \sin[4n\pi v] \\ &= U_{x2} \sin 4\pi v + U_{x4} \sin 8\pi v + \ldots \\ U_{y,z}(v) &= \sum_{n=1} U^S_{(y,z)2n-1} \sin[(4n-2)\pi v] \\ &= U_{(y,z)1} \sin 2\pi v + U_{(y,z)3} \sin 6\pi v + \ldots . \end{aligned}$$

The atoms Sn and Mn2 are at $(0, y, \frac{1}{4})$ in site symmetry $m2m$ with the operations σ_x, C_{2y} and σ_z. The restrictions imposed are

$$\{\sigma_x|000, \tfrac{1}{2}\} \Rightarrow U_x(v) = -U_x(\tfrac{1}{2} - v); \quad U_y(v) = U_y(\tfrac{1}{2} - v)$$
$$\{\sigma_z|00\tfrac{1}{2}, 0\} \Rightarrow U_z(v) = -U_z(v)$$

and so for the U_x modulation odd n allows only cosine terms, while even n allows only sine terms. For U_y the situation is the reverse and for U_z no modulation at all is allowed. The modulation functions hence take the form

$$\begin{aligned} U_x(v) &= \sum_{n=1} U^C_{x(2n-1)} \cos[(4n-2)\pi v] + U^S_{z2n} \sin[4n\pi v] \\ U_y(v) &= \sum_{n=1} U^S_{y(2n-1)} \sin[(4n-2)\pi v] + U^C_{x2n} \cos[4n\pi v] \\ U_z(v) &= 0. \end{aligned}$$

Finally, the occupational probability modulation, $p(v)$, of Mn2 must obey the reflection operation

$$\{\sigma_x|000, \tfrac{1}{2}\} \Rightarrow p(v) = p(\tfrac{1}{2} - v),$$

i.e. the modulation must be mirror symmetric around $v = 0.25$.

The commensurate approximants with $\mathbf{q} = (\frac{3}{5}, 0, 0)$ reduce the distortion to the displacements at a discrete set of points along the internal coordinate of the modulations. As the average coordinate, x, of all atoms is zero and considering our origin choice, this set is formed by the ten values $v_n = 3n/10 \pmod{Z}$ associated with the cells $(n/2, m, p)$ for the *Pbnm* approximant. While, for the *Pmnm* approximation, the realized displacements are those at the v values $v_n = 3n/10 + \frac{1}{4} \pmod{Z}$ for the same cells. As the number of discrete points along the modulation which are physically relevant in each approximant is quite high, and high-order satellites are negligible, the structure refinement within any of the three space groups above is expected to give similar agreement between model and experiment (Pérez-Mato, 1991).

References

Eitel, M. & Bärnighausen, H. (1985). *KA Crystallographic Program. No 5/SFLS. Structure Factors and Least Squares - a Modification of OR-FLS.* Version zur verfeinerung von Datensätzen verzwillingter oder verdrillingter Kristalle. Universität Karlsruhe, Germany.

Elding-Pontén, M., Stenberg, L., Larsson, A.-K., Lidin, S. & Ståhl, K. (1997). *J. Solid State Chem.* In the press.

Larsson, A.-K., Stenberg, L. & Lidin, S. (1994). *Acta Cryst.* **B50**, 636–643.

Lidin, S. & Larsson, A.-K. (1995). *J. Solid State Chem.* **118**, 313–322.

Molecular Structure Corporation (1993). *TEXSAN. Single Crystal Structure Analysis Software*, Version 1.6. MSC, 3200 Research Forest Drive, The Woodlands, TX 77381, USA.

Pérez-Mato, J. M. (1991). *Methods of Structural Analysis of Modulated Structures and Quasicrystals*, edited by J. M. Pérez-Mato, F. J. Zúñiga & G. Madariaga, pp. 117–128. Singapore: World Scientific.

Petříček, V. (1994). *Crystallographic Computing System JANA*. Institute of Physics, Academy of Sciences of the Czech Republic, Prague, Czech Republic.

Petříček, V., van der Lee, A. & Evain, M. (1995). *Acta Cryst.* A**51**, 529–535.

Sheldrick, G. M. (1990). *Acta Cryst.* A**46**, 467–473.

Sheldrick, G. M. (1993). *SHELXL*93. *Program for the Refinement of Crystal Structures*. University of Göttingen, Germany.